A Simple and Practical Spreadsheet-Based Method to Extract Single-Molecule Dissociation Kinetics from Variable Loading-Rate Force Spectroscopy Data

ARTICLE *in* THE JOURNAL OF PHYSICAL CHEMISTRY C · DECEMBER 2008

Impact Factor: 4.77 · DOI: 10.1021/jp806649a · Source: PubMed

6 AUTHORS, INCLUDING:

Robert L Clark
University of Rochester
221 PUBLICATIONS **2,686** CITATIONS

Published in final edited form as:
J Phys Chem C Nanomater Interfaces. 2008 December 11; 112(49): 19163–19167. doi:10.1021/jp806649a.

A Simple and Practical Spreadsheet-Based Method to Extract Single-Molecule Dissociation Kinetics from Variable Loading-Rate Force Spectroscopy Data

Michael J. Serpe[†,§], **Farrell R. Kersey**[†,§], **Jason R. Whitehead**[†,§], **Scott M. Wilson**[‡,§], **Robert L. Clark**[°], and **Stephen L. Craig**[†,§,*]

[†] Department of Chemistry, University of Rochester

[‡] Department of Mechanical Engineering and Materials Science, University of Rochester

[§] Center for Biologically Inspired Materials and Material Systems, University of Rochester

[°] School of Engineering and Applied Sciences, University of Rochester

We report here a simple, practical, and model-free method by which kinetic data can be extracted from variable loading-rate single molecule dynamic force spectroscopy experiments. Dynamic force spectroscopy (DFS) is an increasingly valuable technique that provides the opportunity to probe otherwise inaccessible details of molecular potential energy landscapes.[1–13] In typical DFS experiments using the atomic force microscope (AFM), a molecule is physically tethered between a substrate and a cantilever, as in Figure 1. An increasing force is applied to the tethered molecule by separating the two surfaces, and changes in the molecule (e.g., conformational changes, bond breaking) are inferred as a function of the applied force through the positional changes in the cantilever. To date, DFS has been used to study a multitude of systems/properties, including: protein folding pathways,[14–18] bimolecular substitution reactions,[13] coordination complexes,[13,19] ligand-receptor interactions,[1,2,10,20] DNA base pair interactions,[21–27] polymer conformations,[28–30] supramolecular interactions,[29–34] and hydrophobic interactions.[5]

Broadly, interpreting the results of a DFS experiment often comprises two steps: (1) experimentally determining the dependence of a rate constant (e.g., for bond dissociation) on the applied force, and (2) relating that force dependency to features of a potential energy surface and the stress-free off rate k_d^0. Approaches to the latter step represent an ongoing and vibrant area of research that is beyond the scope of this manuscript.[6,7,9,12,35–38] The first step, i.e. obtaining reliable data for the force-dependent dissociation rate constant $k_d(F)$, is often problematic. The difficulty stems from the fact that the applied force is typically variable and changes substantially over the course of each measurement, while the information that is typically desired is the rate of a process at a constant force. When the change in force with time (often called the force loading rate, $r = dF/dt$) is assumed to be constant, Evans[9] has shown that the most probable rupture force (F^*) depends on the force loading rate according to equation 1:

E-mail: stephen.craig@duke.edu.

Supporting Information. Simulation method, representative time and force histograms, as well as the kinetics fits summarized in Table 1 are provided. This information is available free of charge via the Internet at http://pubs.acs.org.

$$F^*(r_f)=F_\beta \cdot \ln\left(\frac{r_f}{k_d^0 \cdot F_\beta}\right) \quad (1)$$

This model assumes that the force dependency F_β is constant over a range of r_f, where $F_\beta=\frac{k_B T}{x_\beta}$, x_β is the barrier width (distance between equilibrium and the transition state on a potential energy surface projected along the vector of applied force), k_B is Boltzmann's constant, and T is the temperature. Using eq (1), k_d^0 and F_β can be derived by measuring F^* at different r_f. Alternatively, if F_β and r_f are constant, F_β and k_d^0 can be obtained at a single loading rate by fitting the distribution of F^* and r_f. For example, Gaub et al.[12] recently introduced a method to extract k_d^0 and F_β by directly fitting a probability density function to the distributions of bond rupture force and loading rate. Equation 1 has proven to be quite useful in AFM-based DFS experiments, but it becomes mathematically and practically difficult—although not impossible[9,39,40]—to apply to real systems that employ polydisperse polymer tethers to anchor the molecules of interest to the AFM tip and substrate (Figure 1). Polymeric tethers are commonly used to decouple non-specific interactions between the AFM cantilever and substrate from the molecular interaction of interest, and they are typically more compliant than the cantilever itself. As a result, the force loading rate is dynamic and changes with force in a manner that is analytically complex.[39,40] There are further complexities due to the angle at which the molecule is bound to the cantilever from the surface, making the force applied to the bond of interest different depending on this angle.[41] Finally, these treatments typically x_β or other functional forms of the potential energy surface, and the assume constant final force dependency $k_d(F)$ therefore relies on the validity of the chemical logic used to estimate the shape of the potential energy surface in advance.

The difficulties associated with variable loading rates can be avoided experimentally by using force clamping techniques, in which a constant force on a bond is maintained using feedback electronics. Force clamp experiments have been used to directly monitor unfolding/refolding kinetics in proteins and bimolecular reaction kinetics.[42–45] Despite their advantages, for many experiments, force clamping is more difficult to program and execute than constant piezo retraction experiments, and most commercially available AFM software does not offer a force clamping option. As a result, the majority of DFS experiments are conducted under conditions of a variable loading rate.

For practical reasons, the variable loading rate is typically treated as though it were constant. For example, it is often assumed that the loading rate is constant from pull to pull and is the product of the spring constant of the cantilever (N/m) and the retract velocity (m/sec)—the so-called nominal loading rate. Another approach is to assume that the characteristic loading rate for each experiment is the loading rate directly prior to bond rupture.[6,7,12] In this case, a distribution of loading rates is obtained and the peak in that distribution, i.e. the most frequent loading rate, can be used in the subsequent analysis. The force loading rate can also be corrected and predicted by treating the polymeric tether as either a wormlike chain or a freely jointed chain.[39,40] In any of these approaches, the data can be culled to include only a subset of cases in which the assumptions are more likely to be valid.[12,39,40] In this manuscript we present a complementary method for extracting force dependent kinetic data from DFS experiments. This method is direct; it makes no assumptions regarding the form of the loading rate, or even whether the force loading profile is the same from one experiment to another. It is also conceptually simple and easy to implement, and it therefore has both practical and theoretical advantages over previously reported methods.

Fundamentally, $k_d(F)$ is defined as the probability of an event (e.g., bond rupture) over a given time interval at a given force. Experimentally, this probability is related to an observed event frequency (equation 2):

$$k_d^*(F)=\frac{N(F)}{t(F)}, \tag{2}$$

where $k_d^*(F)$ is the experimentally-determined, force-dependent event frequency (e.g., the Bell off rate constant), $N(F)$ is the number of events that occur at a given force F, and $t(F)$ is the time that the bond resides at that force. We point out here that $N(F)$ and $t(F)$ are also easily extracted under the variable force conditions of a DFS experiment.

Constructing histograms of force-dependent events as a function of force interval, $N(F, F+\Delta F)$, is a routine part of most DFS data interpretation, either by inspection or by applying a set of objective, analytical criteria. In contrast, $t(F)$ is usually not determined directly, but rather a set of data is interpreted on the basis of an approximated force vs. time history, e.g. constant loading rate.[5,46] In fact, $t(F)$ is effectively recorded directly in a DFS experiment and can be used as such without any approximation regarding the actual force vs. time history of a series of experiments. In a typical DFS experiment, using digital data acquisition, data points are obtained at a fixed sampling rate v, and so force measurements are acquired at evenly spaced time intervals $t_{acq} = 1/v$. Because the sampling rate v is typically fast relative to the change in force, each recording of a force value F represents an additional increment of t_{acq} to the total time $t(F)$ that the molecule of interest experienced that force.

It is therefore straightforward to determine directly the time spent in a given range of forces, $t(F, F+\Delta F)$, which is simply the number of data points that fall between F and $F+\Delta F$, multiplied by t_{acq}. This process is illustrated in Figure 2(a and b). This analysis is completed easily using histogram functions on any of a number of commercially available spreadsheet programs. An immediate advantage is that *all* force curves for a single molecular event of interest can be combined, regardless of the changes in loading rate due to, e.g., variations in pulling speed and/or polymer tether length or compliance. Subsequently, the forces at which a given conformational change or bond rupture event occur can be similarly tabulated and binned according to the same force intervals as the force history data, as seen in Figure 2(c). Dividing $N(F, F+\Delta F)$ by $t(F, F+\Delta F)$, in Figures 2 (c) and 2 (b) respectively, gives $k_d^*(F, F+\Delta F)$, which can be plotted as a function of force, as in Figure 2(d).

In effect, what the histogram/binning process does is to turn a set of variable force data into a new set of (nearly) constant force data. The process is effectively the reverse of Monte Carlo simulations of stochastic bond rupture,[12] and it is facilitated by the constant-interval digital data acquisition. Once collected, a set of data can be collated into any of a number of sets of force bins (variable sizes and numbers of bins). These intervals of "constant" force can be as small as desired, although there would seem to be little benefit for $\Delta F <$ thermal noise of the cantilever.

The efficacy of the method is demonstrated by applying it to a set of model data (Table 1), generated using stochastic computer simulations of bond rupture in a freely jointed chain (FJC) polymer (contour length = 40 nm, Kuhn length = 0.7 nm). A few points bear emphasizing. First, the derived rate vs. force data, including the extrapolated stress-free rate constant k_d^0, are in excellent agreement with the force dependency used to generate the data. In fact, the kinetics derived from data obtained at a single loading rate using the histogram binning method presented here are more accurate than those derived from a combined set of data at six different loading rates using eq (1). Second, high-quality kinetic information can be derived even from

data that is problematic to include in an analysis using eq (1). Rupture force histograms often lack a clear F^*, as demonstrated by the computer simulations of stochastic rupture at a tip retract velocity of 125 nm s^{-1} (Figure SI-1). Identifying the most probable rupture force in such cases is problematic and depends on a valid model for the rupture force distribution under the variable loading rate conditions of the experiment. No such model is needed to obtain the kinetics reported in Table 1.

This method can be extended to data from the opening of multiple identical bonds in series with minimal modification of the analysis, as shown in Figure 3. For example, if there are three stress-bearing bonds in series, the applied force is felt equally by the three bonds (assuming the geometry of attachment is identical). So, prior to the first rupture event, three bonds are feeling the same force in each acquisition interval t_{acq}, which translates to a single bond feeling that force for $3 \times t_{acq}$. Thus, each of the data points prior to the first rupture should be counted three times. Following the first rupture, the applied force is felt by only the two bonds left in series, and each data point needs to be counted twice. The remaining extension curve can now be treated normally.

The treatment described above relies on the same underlying physics established previously, [9] but has many practical advantages when it comes to implementation. For example, the proposed method allows kinetic data to be extracted from traditional DFS experiments, and, unlike commonly employed methods, data can be taken at either a single nominal loading rate or multiple loading rates, without actually characterizing those loading rates. Further, the method is insensitive to polymer tether polydispersity, since the data is extracted directly from force curves with no assumptions. The ease of analysis lies in the ability to use any of a number of seemingly ubiquitous spreadsheet programs, to integrate data from multiple sets that have the same sampling rate, regardless of differing loading rates between sets, and the fact that no functional form of the potential energy surface (x_β) need be assumed in order to determine $k_d^*(F)$. Once the data are in hand, however, $k_d^*(F)$ can be interpreted in terms of various models for reaction potential energy surfaces[6,7,9,12,35–38] (as done here for the Bell-Evans case).

Several points should be considered when using the method presented here. First, while thermal noise in the cantilever is largely taken into account, noise in the detector can bias the measurements by incorrectly reporting $t(F)$. The effect of random noise in the detector can often be reduced by signal averaging, but nonetheless an analysis of simulations that include detector noise (Gaussian white noise, standard deviations of 2, 5, and 10 pN) gave values for k_d^0 and F_β that are as accurate, or more so, than the values derived using eq (1) under noise-free conditions (see Supporting Information). Second, the lower "force limit" (see Figure 2(a)) used to generate the $t(F, F+\Delta F)$ histograms should be chosen so that events that occur at or above the force limit are observable. Finally, unlike methods that rely on the "most probable" force, the results of the present treatment depend on *all* data that are obtained in a set of experiments. As such, it is more sensitive to the presence of a small number of "false data", e.g. trace impurities, and/or the simultaneous rupture of multiple bonds in parallel. Such data would have a much smaller impact on analyses based on the peak in a distribution. This consideration is also important in treatments based on distribution fitting,[12] and it is certainly not prohibitive. As such, we believe that the simple analysis method presented here will be operationally useful in the analysis of many DFS experiments.

Supplementary Material

Refer to Web version on PubMed Central for supplementary material.

Acknowledgments

This material is based on work supported by the U.S. Army Research Office under grant W911NF-07-1-0409. Partial support was provided by NIH grant EB-001307. JRW acknowledges the support of a Duke GPNANO fellowship and NIH predoctoral traineeship (GM85555). SMW and RLC thank the NSF (IGERT Grant DGE-0221632) for funding.

References

1. Florin EL, Moy VT, Gaub HE. Adhesion Forces between Individual Ligand-Receptor Pairs. Science 1994;264:415–417. [PubMed: 8153628]
2. Moy VT, Florin EL, Gaub HE. Intermolecular Forces and Energies between Ligands and Receptors. Science 1994;266:257–259. [PubMed: 7939660]
3. Lee GU, Chrisey LA, Colton RJ. Direct Measurement of the Forces between Complementary Strands of DNA. Science 1994;266:771–773. [PubMed: 7973628]
4. Ray C, Akhremitchev BB. Conformational heterogeneity of surface-grafted amyloidogenic fragments of alpha-synuclein dimers detected by atomic force microscopy. J Am Chem Soc 2005;127:14739–14744. [PubMed: 16231928]
5. Ray C, Brown JR, Akhremitchev BB. Single-molecule force spectroscopy measurements of "hydrophobic bond" between tethered hexadecane molecules. J Phys Chem B 2006;110:17578–17583. [PubMed: 16942101]
6. Evans E. Probing the relation between force - Lifetime - and chemistry in single molecular bonds. Annu Rev Biophys Biomolec Struct 2001;30:105–128.
7. Evans E. Energy landscapes of biomolecular adhesion and receptor anchoring at interfaces explored with dynamic force spectroscopy. Faraday Discuss 1998:1–16. [PubMed: 10822596]
8. Evans E, Ritchie K. Strength of a weak bond connecting flexible polymer chains. Biophys J 1999;76:2439–2447. [PubMed: 10233061]
9. Evans E, Ritchie K. Dynamic strength of molecular adhesion bonds. Biophys J 1997;72:1541–1555. [PubMed: 9083660]
10. Merkel R, Nassoy P, Leung A, Ritchie K, Evans E. Energy landscapes of receptor-ligand bonds explored with dynamic force spectroscopy. Nature 1999;397:50–53. [PubMed: 9892352]
11. Schmidt SW, Beyer MK, Clausen-Schaumann H. Dynamic strength of the silicon-carbon bond observed over three decades of force-loading rates. J Am Chem Soc 2008;130:3664–3668. [PubMed: 18302382]
12. Friedsam C, Wehle AK, Kuhner F, Gaub HE. Dynamic single-molecule force spectroscopy: bond rupture analysis with variable spacer length. J Phys -Condes Matter 2003;15:S1709–S1723.
13. Kersey FR, Yount WC, Craig SL. Single-molecule force spectroscopy of bimolecular reactions: System homology in the mechanical activation of ligand substitution reactions. J Am Chem Soc 2006;128:3886–3887. [PubMed: 16551077]
14. Carrion-Vazquez M, Oberhauser AF, Fowler SB, Marszalek PE, Broedel SE, Clarke J, Fernandez JM. Mechanical and chemical unfolding of a single protein: A comparison. Proc Natl Acad Sci U S A 1999;96:3694–3699. [PubMed: 10097099]
15. Oberhauser AF, Marszalek PE, Erickson HP, Fernandez JM. The molecular elasticity of the extracellular matrix protein tenascin. Nature 1998;393:181–185. [PubMed: 9603523]
16. Rief M, Gautel M, Oesterhelt F, Fernandez JM, Gaub HE. Reversible unfolding of individual titin immunoglobulin domains by AFM. Science 1997;276:1109–1112. [PubMed: 9148804]
17. Bustanji Y, Samori B. The mechanical properties of human angiostatin can be modulated by means of its disulfide bonds: A single-molecule force-spectroscopy study. Angew Chem-Int Edit 2002;41:1546–1548.
18. Williams PM, Fowler SB, Best RB, Toca-Herrera JL, Scott KA, Steward A, Clarke J. Hidden complexity in the mechanical properties of titin. Nature 2003;422:446–449. [PubMed: 12660787]
19. Kudera M, Eschbaumer C, Gaub HE, Schubert US. Analysis of metallo-supramolecular systems using single-molecule force spectroscopy. Adv Funct Mater 2003;13:615–620.
20. Neuert G, Albrecht C, Pamir E, Gaub HE. Dynamic force spectroscopy of the digoxigenin-antibody complex. FEBS Lett 2006;580:505–509. [PubMed: 16388805]

21. Albrecht C, Blank K, Lalic-Multhaler M, Hirler S, Mai T, Gilbert I, Schiffmann S, Bayer T, Clausen-Schaumann H, Gaub HE. DNA: A programmable force sensor. Science 2003;301:367–370. [PubMed: 12869761]
22. Kersey FR, Lee G, Marszalek P, Craig SL. Surface-to-surface bridges formed by reversibly assembled polymers. J Am Chem Soc 2004;126:3038–3039. [PubMed: 15012119]
23. Kuhner F, Morfill J, Neher RA, Blank K, Gaub HE. Force-induced DNA slippage. Biophys J 2007;92:2491–2497. [PubMed: 17218463]
24. Morfill J, Kuhner F, Blank K, Lugmaier RA, Sedlmair J, Gaub HE. B-S Transition in Short Oligonucleotides. Biophys J 2007;93:2400–2409. [PubMed: 17557787]
25. Lee G, Rabbi M, Clark RL, Marszalek PE. Nanomechanical fingerprints of UV damage to DNA. Small 2007;3:809–813. [PubMed: 17393552]
26. Pope LH, Davies MC, Laughton CA, Roberts CJ, Tendler SJB, Williams PM. Force-induced melting of a short DNA double helix. Eur Biophys J 2001;30:53–62. [PubMed: 11372533]
27. Serpe MJ, Rivera M, Kersey FR, Clark RL, Craig SL. Time and Distance Dependence of Reversible Polymer Bridging Followed by Single-Molecule Force Spectroscopy. Langmuir 2008;24:4738–4742. [PubMed: 18348580]
28. Oesterhelt F, Rief M, Gaub HE. Single molecule force spectroscopy by AFM indicates helical structure of poly(ethylene-glycol) in water. New J Phys 1999 ;1:6.1–6.11.
29. Guan ZB, Roland JT, Bai JZ, Ma SX, McIntire TM, Nguyen M. Modular domain structure: A biomimetic strategy for advanced polymeric materials. J Am Chem Soc 2004;126:2058–2065. [PubMed: 14971940]
30. Roland JT, Guan ZB. Synthesis and single-molecule studies of a well-defined biomimetic modular multidomain polymer using a peptidomimetic beta-sheet module. J Am Chem Soc 2004;126:14328–14329. [PubMed: 15521732]
31. Embrechts A, Schonherr H, Vancso GJ. Rupture force of single supramolecular bonds in associative polymers by AFM at fixed loading rates. J Phys Chem B 2008;112:7359–7362. [PubMed: 18512892]
32. Vancso GJ. Feeling the force of supramolecular bonds in polymers. Angew Chem-Int Edit 2007;46:3794–3796.
33. Zou S, Schonherr H, Vancso GJ. Stretching and rupturing individual supramolecular polymer chains by AFM. Angew Chem-Int Edit 2005;44:956–959.
34. Eckel R, Ros R, Decker B, Mattay J, Anselmetti D. Supramolecular chemistry at the single-molecule level. Angew Chem-Int Edit 2005;44:484–488.
35. Bell GI. Models for Specific Adhesion of Cells to Cells. Science 1978;200:618–627. [PubMed: 347575]
36. Best RB, Hummer G. Protein folding kinetics under force from molecular simulation. J Am Chem Soc 2008;130:3706–3707. [PubMed: 18307341]
37. Dudko OK, Filippov AE, Klafter J, Urbakh M. Beyond the conventional description of dynamic force spectroscopy of adhesion bonds. Proc Natl Acad Sci U S A 2003;100:11378–11381. [PubMed: 13679588]
38. Hummer G, Szabo A. Kinetics from nonequilibrium single-molecule pulling experiments. Biophys J 2003;85:5–15. [PubMed: 12829459]
39. Ray C, Brown JR, Akhremitchev BB. Rupture force analysis and the associated systematic errors in force spectroscopy by AFM. Langmuir 2007;23:6076–6083. [PubMed: 17439260]
40. Ray C, Brown JR, Akhremitchev BB. Correction of systematic errors in single-molecule force spectroscopy with polymeric tethers by atomic force microscopy. J Phys Chem B 2007;111:1963–1974. [PubMed: 17284065]
41. Ke CH, Jiang Y, Rivera M, Clark RL, Marszalek PE. Pulling geometry-induced errors in single molecule force spectroscopy measurements. Biophys J 2007;92:L76–L78. [PubMed: 17324999]
42. Ainavarapu SRK, Wiita AP, Dougan L, Uggerud E, Fernandez JM. Single-Molecule Force Spectroscopy Measurements of Bond Elongation during a Bimolecular Reaction. J Am Chem Soc 2008;130:6479–6487. [PubMed: 18433129]
43. Schlierf M, Li HB, Fernandez JM. The unfolding kinetics of ubiquitin captured with single-molecule force-clamp techniques. Proc Natl Acad Sci U S A 2004;101:7299–7304. [PubMed: 15123816]

44. Wiita AP, Ainavarapu SRK, Huang HH, Fernandez JM. Force-dependent chemical kinetics of disulfide bond reduction observed with single-molecule techniques. Proc Natl Acad Sci U S A 2006;103:7222–7227. [PubMed: 16645035]

45. Garcia-Manyes S, Brujic J, Badilla CL, Fernandez JM. Force-clamp spectroscopy of single-protein monomers reveals the individual unfolding and folding pathways of I27 and ubiquitin. Biophys J 2007;93:2436–2446. [PubMed: 17545242]

46. Strunz T, Oroszlan K, Schafer R, Guntherodt HJ. Dynamic force spectroscopy of single DNA molecules. Proc Natl Acad Sci U S A 1999;96:11277–11282. [PubMed: 10500167]

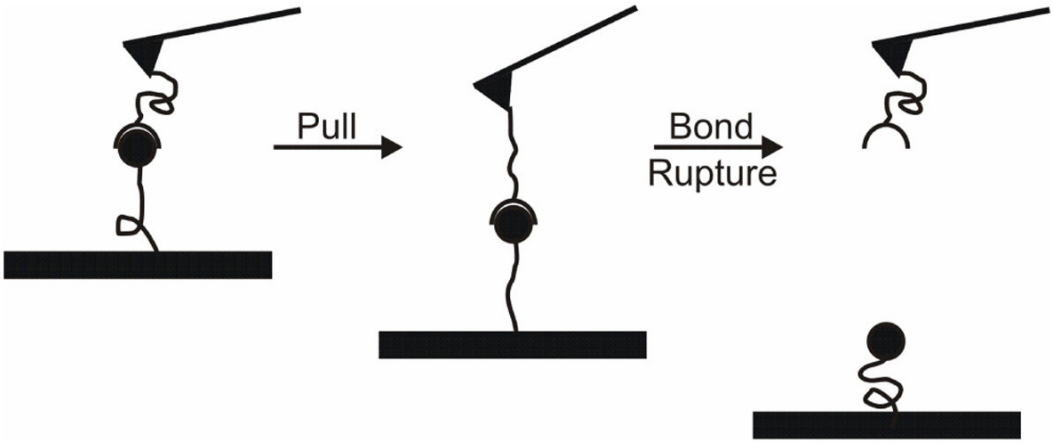

Figure 1.
Example of a single bond tethered between an AFM cantilever and a substrate. Force is applied to the bond by retracting the substrate from the tip so that the force increases until the bond breaks.

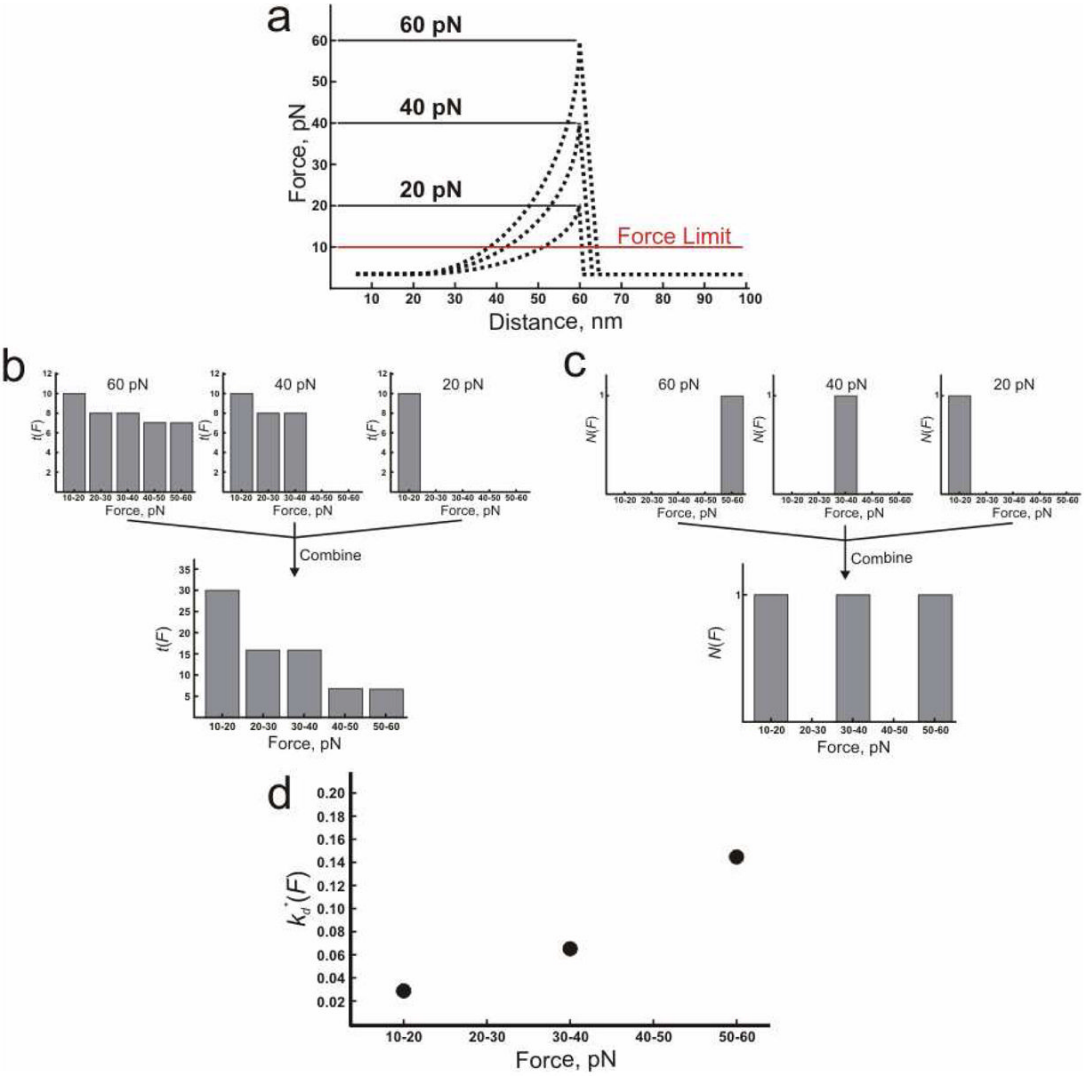

Figure 2.

(a) Pictorial representation of AFM pulling data; data are for illustration only and do not reflect an actual experiment or simulation. The force offset (from 0 pN) is included for visual clarity. Here, a single bond is tethered between an AFM tip and substrate and force is applied at some rate. A force measurement is taken at the sampling rate of the experiment (v) and is represented as individual points on the plot. Each point is indicative of a time the bond felt the indicated force. (b) For each of the events in (a) a histogram is made of the number of points that are contained in a predetermined force range that is above the force limit up to the actual rupture event. In this example, the force intervals are set to 10 pN. The number of points in each force interval can easily be converted to time at that force $t(F)$ by multiplying the number of points by $1/v$.(b, bottom) The times each bond spent at each force are then combined to make one histogram. (c) For each of the events in (a) a histogram is made of the rupture forces using the same force bin width as in (b). (c, bottom) All rupture forces are collected into one histogram. (d) All $t(F)$ and $N(F)$ are used to calculate $k_d^*(F)$ and is plotted as a function of the force bin width.

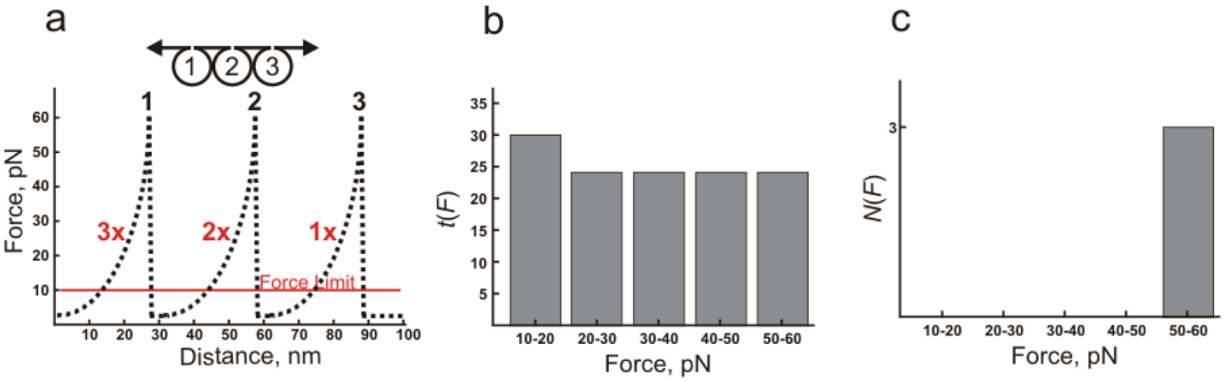

Figure 3.

(a) Pictorial representation of AFM pulling data that may be obtained by pulling on bonds in series; data are for illustration only and do not reflect an actual experiment or simulation. Since there are three bonds in series, prior to the first rupture three bonds are feeling the force. Therefore, the time spent up to the first rupture needs to be multiplied by three. Similarly, the time spent applying a force up until the second rupture needs to be multiplied by two. The remaining bond can be treated as usual. (b) All the times that a bond felt force, corrected for the number of bonds in series, are collected into a histogram. (c) Similarly, a histogram of all the rupture forces is made. Combining the data from (b) and (c) gives values for $k_d^*(F)$.

Table 1

Comparison of the kinetic parameters obtained using the method proposed here (top of table) and the Bell-Evans model (bottom of table). For the Bell-Evans fit, r_f was assumed to be constant and is the product of the retract velocity and the spring constant of the cantilever (40 pN/nm). Parameters: $k_d^0 = 1\ s^{-1}$, F_β = 22.5 pN, and the standard deviation of Gaussian white thermal noise in the cantilever = ± 10 pN.

Retract Velocity (nm s^{-1})	F^*(pN)	k_d^0 (s^{-1})	F_β (pN)
37.5	55	0.79	22.5
125	105	1.5	24.8
375	115	0.59	20.3
1250	175	0.73	23.6
3750	185	0.88	23.5
12500	195	0.66	23.3
From eq (1)		4.1	24.8